HEAT TRANSFER ENHANCEMENT THROUGH PCM THERMAL STORAGE BY USE OF COPPER FINS

by

Nedžad R. RUDONJA[a*], Mirko S. KOMATINA[a], Goran S. ŽIVKOVIĆ[b], and Dragi Lj. ANTONIJEVIĆ[c]

[a] Faculty of Mechanical Engineering, University of Belgrade, Belgrade, Serbia
[b] Laboratory for Thermal Engineering and Energy, Vinca Institute of Nuclear Sciences, University of Belgrade, Belgrade, Serbia
[c] Faculty of Applied Ecology, Singidunum University, Belgrade, Serbia

Original scientific paper
DOI: 10.2298/TSCI150729136R

Enhancement of heat transfer over a cylinder shaped thermal energy storage filled by paraffin E53 by use of longitudinal rectangular copper fins was analyzed. The thermo-physical features of the storage material are determined in separate experiments and implemented to FLUENT software over user defined function. Advanced thermal storage geometry comprehension and optimization required introduction of a parameter suitable for the analysis of heat transfer enhancement, so the ratio of heat transfer surfaces as a factor was proposed and applied. It is revealed that increase of the ratio of heat transfer surfaces leads to the decrease of melting time and vice versa. Numerical analysis, employing the 3-D model built in Ansys software, observed storage reservoir geometries with variable number of longitudinal fins. The adjusted set of boundary conditions was carried out and both written in C language and implemented over user defined function in order to define variable heat flux along the height of the heater. The comparison of acquired numerical and experimental results showed a strong correlation. Experimental validation of numerical results was done on the real thermal energy storage apparatus.

Key words: *thermal energy storage, phase change material, paraffin, numerical modeling*

Introduction

Thermal energy storage (TES) is an important part of an efficient thermal engineering system. It has been used for eliminating the mismatch between energy supply and energy demand. Furthermore, TES contributes to the lower investment and operational cost (decreasing installed power) of the plants as well as reducing of environmental impacts.

Mainly two types of TES have been used: sensible and latent. Latent TES has gained more attention as result of the fact that materials used for storing energy have nearly constant phase change temperature and high density of stored energy per unit of volume [1, 2]. Nevertheless, materials that have been used in latent TES, phase change material (PCM) have limited application due to their low thermal conductivity. This disadvantage lengthens the melting time of PCM as well as its solidification time.

There are few possible approaches for overcoming the problem of low thermal conductivity. A common solution is inserting high conductivity materials in shape of grains or

* Corresponding author; e-mail: nrudonja@mas.bg.ac.rs

small particles into PCM. The result is heat transfer enhancement by approximately 60-150% [3]. However, the main problem of the method is deposition of inserted materials with the time as the result of acting gravitational force. Some researchers [4, 5] explored use of metal foams as the structure whose pores are filled by PCM. Achieved heat transfer enhancement is from 3-10 times. On the other hand, the main disadvantage of this method is sub-cooling of PCM as result of increased flow resistance.

Finally, the most proposed method suggests utilization of metal fins. The metal fins play the role of thermal bridges in PCM [6]. Mosaffa *et al.* [7] developed an analytical 2-D model as well as numerical model of the solidification process for prediction of temperature distribution inside a thermal storage container with rectangular horizontal fins. They used constant convective heat transfer coefficient and constant temperature along storage walls. The main conclusion was that reduction in total solidification time due to the decrease in the inlet temperature of heat transfer fluid was significant. Al-Abbidi *et al.* [8] developed a 2-D model with internal and external fins. They analyzed influence of fins length, number, thickness as well as material of fins to the melting time. It was concluded that fins thickness has negligible influence to the melting time comparing to the fin's length and number.

However, many articles that have been published the heat transfer enhancement was tracked down based on the number of fins or the fin dimensions [7, 9, 10]. However, for design and optimization of real TES apparatus it is more convenient to introduce a geometric parameter that can unify all fin dimensions. For this reason in the present paper the heat transfer enhancement was tracked down through a geometric parameter that represents the ratio of the heat transfer surfaces. The paraffin E53 (commercial-grade wax) was selected as a working medium because of the fact that such organic materials have nearly constant temperature of the phase change as well as due to low value of oil content (high resistance to explosion). Since the accurate determination of thermo-physical properties of the PCM is essential for numerical simulation of TES they were determined by measurements.

Thermo-physical properties of working medium

To obtain thermal properties of E53 differential scanning calorimeter (DSC) was used. The measurements were conducted on DSC EVO 131 apparatus in order to obtain latent heat of phase change as well as the specific heat capacity dependence on temperature. Figure 1 shows results obtained during continuous measuring of thermal properties of the paraffin E53. The mass of the sample was 7.2 kg^{-6}. Apparently, there are two peaks as a consequence of presence of more than one fraction in the paraffin. The start of the smaller peak corresponds to the solidus curve where the melting process begins while the end of the bigger peak corresponds to the liquids curve where the melting process ends. As a consequence of the presence of two peaks the total latent heat is the sum of the latent heats, *i. e.* 155931 J/kg.

Thermal conductivity of the paraffin E53 was determined by C-therm analyzer. The results are shown in fig. 2. The peaks have the same cause as in the case of the specific heat capacity measurement.

The functional dependencies the thermo-physical properties of the paraffin listed in tab. 1 were used for numerical simulations and implemented to FLUENT model by the user defined function (UDF).

Physical model

The physical model consists of a central positioned electric heater inserted in the inner cylinder, fins, and outer cylinder. A radial cross-section of the TES considered in present

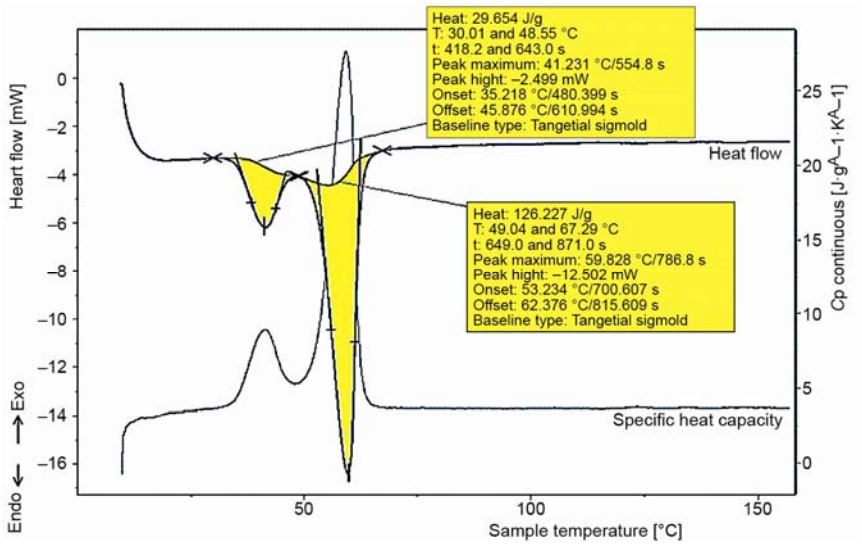

Figure 1. The DSC heating curves of paraffin E53

study is shown in fig. 3. Cooper fins (1) are evenly arranged and welded along the inner cylinder (3). Inside the cylinder (3) the electric heater with the total power input 2400 W is placed. The space between the cooper fins, inner and outer cylinder (4) is filled by paraffin E53 as working medium (2). Total height of fins, cylinders and PCM is 500 mm, while other dimensions are shown in fig. 3.

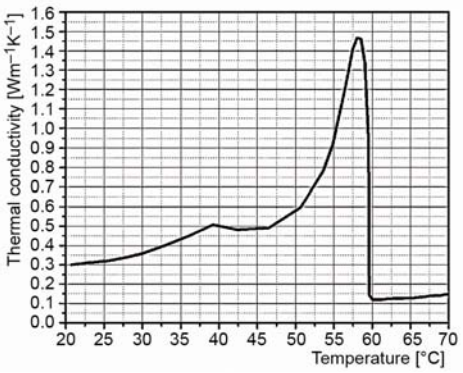

Figure 2. Thermal conductivity of E53

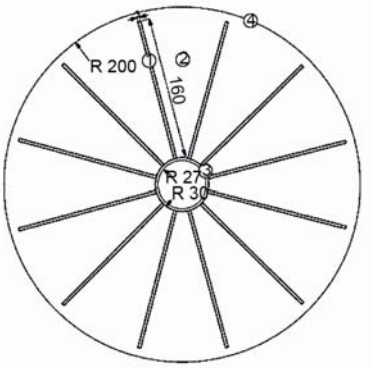

Figure 3. Physical model of the TES with 12 cooper fins: (1) fin, (2) PCM, (3) iner cylinder, and (4) outer cylinder

Three basic lay-outs cases were analyzed: I – heating cylinder without fins, II – with six identical longitudinal fins, and III – with twelve identical longitudinal fins.

Observing the heat transfer enhancement using only fins dimensions is not only complicated procedure, but can be misleading in terms of design conclusions and it is not useful in engineering usage as well. It is more practical to use some geometric ratio which

Table 1. Properties of paraffin E53 used for numerical simulation

Property	Solid	Liquid
Density, ρ [kgm^{-3}]	902	849.6 – 0.2 T
Specific heat capacity, c_p [Jkg^{-1}K^{-1}]	3000	3000
Thermal conductivity, k [Wm^{-1}K^{-1}]	0.01008 T – 2.68425	0.00286 T – 0.83629
Viscosity, μ [Pa·s]		0.001 exp (–4.25 + 1790/T) [11]
Latent heat, L [Jkg^{-1}]	155931	
Solidus temperature, T_s [K]	303	
Liquidus temperature, T_l [K]	340	

includes all fins dimensions. Let the γ be a ratio of heat transfer surfaces, defined as ratio of the overall heat transfer surface for fined surface (case II or III) and the heat transfer surface without fins (case I). In the case that fins are rectangular with the negligible thickness and with the negligible thickness of inner cylinder, γ becomes:

$$\gamma = \frac{n(2l_f Z_f + 2l_f s + 2Z_f s) + d\pi l_f - nsl_f}{d\pi l_f} \tag{1}$$

where n is the number of fins, Z_f – the height of the fin, 160 mm, s – the fin thickness, 3 mm, l_f – the length, 500 mm, d – the outer diameter of the inner cylinder, 60 mm. The calculated surface ratio γ for the cases I, II and III is 1, 11.3, and 21.7, respectively.

Governing equations

Governing equations for 3-D melting and solidification problem are given.

Continuity equation:

$$\frac{\partial}{\partial t}(\rho) + \nabla(\rho\vec{v}) = 0 \tag{2}$$

where ρ is the PCM density and $\vec{v}$ is the velocity vector.

Momentum equation:

$$\frac{\partial}{\partial t}(\rho\vec{v}) + \nabla(\rho\vec{v}\vec{v}) = -\nabla p + \nabla\boldsymbol{\tau} + \rho\vec{g} + S_M \tag{3}$$

where p is the static pressure, $\boldsymbol{\tau}$ is the stress tensor, and S_M is the momentum source term. The enthalpy-porosity approach proposed by Brent *et al.* [12] treats the mushy zone as a porous medium. The porosity in each cell is assumed to be equal to the liquid fraction of that cell. The momentum source term in eq. (3) includes reduced porosity in the mushy zone takes the form:

$$S_M = \frac{(1-\beta)^2}{\beta^3 + 0.001} A_{mush}\vec{v} \tag{4}$$

where β is the liquid volume fraction and A_{mush} is the mushy zone constant. The liquid fraction is defined based on the PCM temperature:

$$\beta = 0, \; T < T_s$$
$$\beta = \frac{T - T_s}{T_l - T_s}, \quad T_s < T < T_l \tag{5}$$
$$\beta = 1, \quad T_l < T$$

where T_s and T_l are solidus and liquidus temperatures, respectively.

Energy equation:

$$\frac{\partial}{\partial t}(\rho H) + \nabla(\rho \vec{v} H) = \nabla(k \nabla T) + \Phi \tag{6}$$

where H is the enthalpy, T – the thermodynamic temperature, and Φ – the energy of dissipation. The enthalpy of PCM is calculated as the sum of the sensible enthalpy, h and the latent heat content, ΔH:

$$H = h + \Delta H \tag{7}$$

$$\Delta H = \beta L \tag{8}$$

Numerical simulations

Set-up procedure

Numerical modeling of phase change processes was carried out by FLUENT software that uses finite volume method for solving continuity, momentum, and energy equations. The procedure of solving those equations by finite volume method was established by Patankar [13]. The coupling between pressure and velocity was conducted by the semi-implicit pressure--linked equation (SIMPLE) algorithm [13]. The PRESTO [13] scheme was used for discretization of the pressure correction equation, while for the momentum and energy equations the first order upwind discretization scheme was used. It was assumed there was no volume change of the paraffin with temperature, its flow through the reservoir during the process was laminar and the energy of dissipation was neglected. Since the shape of TES is cylindrical, the computational domain was divided to two symmetrical halves and thus only a half of the volume was observed. The physical model and the mesh were generated in Ansys software and in each case domain was divided to approximately 45000 cells. In order to achieve convergence at each time step, the time step was set at 1 second. Number of iterations per each time step was 50. The convergence criterion was that the scaled residuals are less than 10^{-4} for the continuity and momentum equation as well as the residual was 10^{-6} for the energy equation. The values of under relaxation factors for pressure, density, body forces, momentum, liquid fraction and energy were 0.3, 1, 1, 0.2, 0.9, and 1, respectively. A personal computer with an Intel Core i5 processor (3.2 GHz) and 16 GB random access memory was used.

The PCM was initially solid at temperature 285 K. The mushy zone constant was set as default value 10^5. The adiabatic thermal condition was applied for the storage walls by setting the zero heat flux through the walls. Heat was entering the domain through the inner radial side of the domain, which was simulated by the electrical heater. The non-slip condition was imposed at all surface walls. In order to get variable heat flux along heater, the special program was written in C language. The surface heat flux equation and its coefficients were determined basing on the temperature profile recorded during experimental measurements with the thermocouples placed at the heater surface. The variable surface heat flux along the height of the heater was given in the form:

$$\dot{q} = 21000 - 64000\frac{\exp(-5.322z) - 1}{5.322} \text{ W/m} \tag{9}$$

where $\dot{q}$ is the surface heat flux and z is the height of the heater.

The switch off temperature sensor was also included in the UDF and geometrically placed as the real control sensor. Thermodynamic properties of E53 were implemented to FLUENT 14.5 software over UDF function.

Numerical results

Figures 4 and 5 show temperature fields inside the TES after 60 and 120 minutes of charging, respectively. Increasing the number of fins results in more intense heat transfer throughout the reservoir and increase the liquid fraction of PCM and thereby causing the decrease of the charging time.

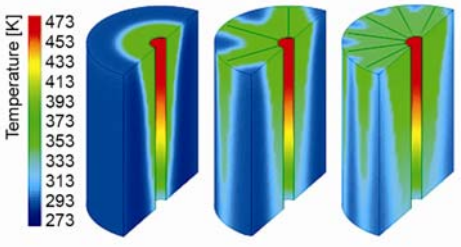

Figure 4. Temperature field inside the TES after 60 min – Case I (left), Case II (middle), and Case III (right)

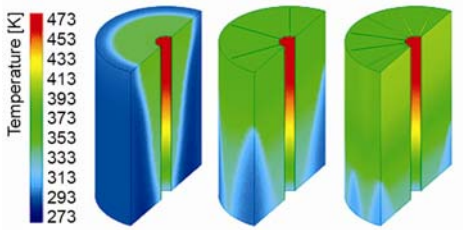

Figure 5. Temperature field inside the TES after 120 min – Case I (left), Case II (middle), and Case III (right)

During the numerical simulation the information about the liquid fraction was recorded and the curve that represents dependence of the melting time of PCM on time created. Liquid fraction inside the TES for all cases after 120 minutes is shown in fig. 6.

Based on the melting time obtained by numerical simulations of the three cases the dependence of melting time from the ratio of heat transfer surfaces can be derived (fig. 7).

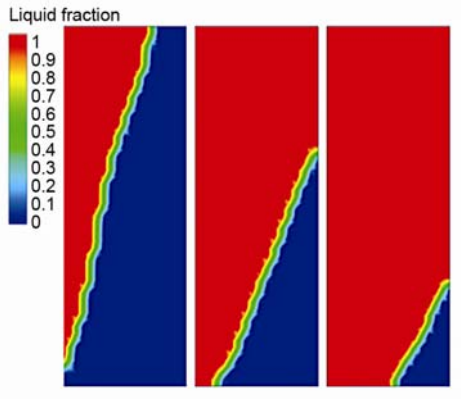

Figure 6. Liquid fraction of PCM after 120 min – Case I (left), Case II (middle), and Case III (right)

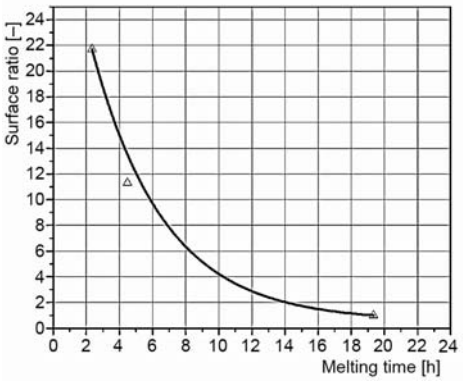

Figure 7. The influence of surface ratio factor to the melting time of PCM

This dependence/correlation can be used for engineering calculations and it is valid for the PCM and known temperature of the heating source and best exemplifies importance application of the ratio of heat transfer surfaces. It is important to emphasize that the surface ratio includes all dimensions of fins and takes into account their influence to the melting/solidification time. As it was expected the melting time of PCM decreases with the increase of the surface ratio. For given geometry of a TES and known the ratio of heat transfer surfaces the melting time of the PCM can be obtained. For instance, if the charging time of a TES is known, the curve of fig. 7. Can be used for the design and optimization of the TES.

Experimental set-up and validification of numerical simulations

In order to verify obtained numerical results experimental investigation was carried out. The experiments were conducted on the experimental installation shown in fig. 8. The main part was the cylindrically shaped tank of about 77 dm^3, whose internal space in this case was filled by paraffin E53 as PCM. The PCM was heated by the electric heater (EH), located in the central position of the TES. Four thermocouples (A1, A2, A3, and A4) were placed at the heater surface. The top thermocouple (A1) at the heater surface was used for the heating control (the switch off sensor). If the temperature of the heater reached 473 K the electricity was switched off, until the temperature dropped below the given range. For the measurement of temperature profile inside PCM, eight thermocouples (B1-B4 and C1-C4) were placed inside the tank, four along the axis and two along the radius. Four thermocouples (D1-D4) were placed at the outer surface of the tank. The enumeration and position are shown in fig. 8.

The frequency of the stored temperature values was each 60 second, which was precise enough for the relatively small change of the temperature field inside the TES. Experimental

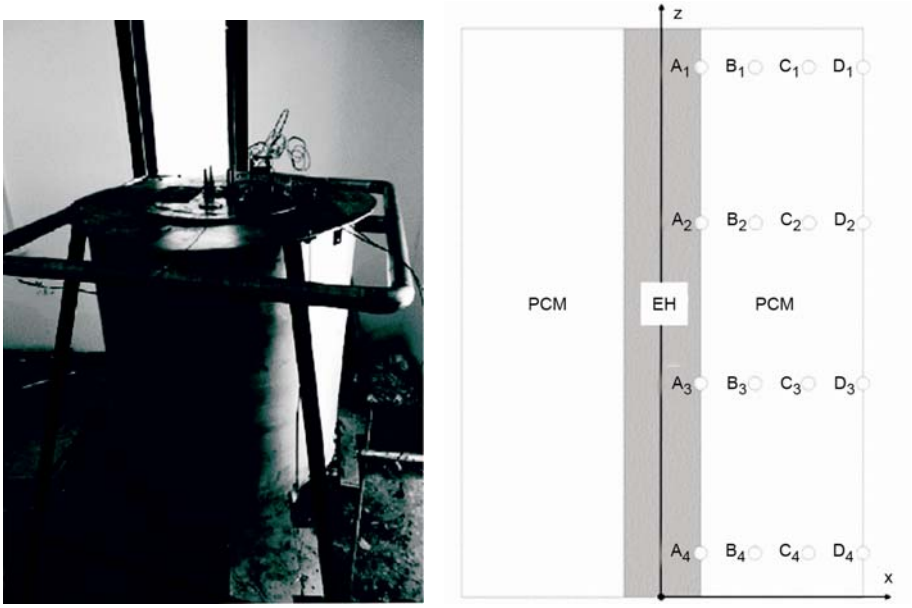

Figure 8. Experimental set-up and position of thermocouples

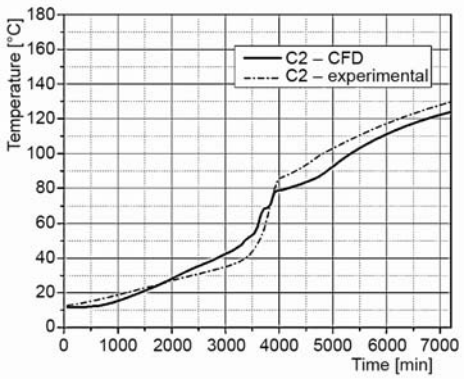

Figure 9. Experimental validification of numerical results

validification of numerical modeling was done by tracking and comparing temperature at the position of the thermocouple C2. This thermocouple was selected as result of the fact that has central position in the TES, but also results from rest of thermocouples were satisfied.

Figure 9 shows the comparison of the numerical and experimental results. The comparison of acquired numerical and experimental results showed a strong correlation.

Conclusions

The utilized numerical procedure for determination of heat transfer processes in the TES is very sensitive to the storage material thermo-physical properties, hence the exact values of specific heat capacity, thermal conductivity and density of paraffin E53 were obtained experimentally, using a DSC analysis, thermal conductivity analyzer and density measurements. It has been detected that there are significant variations of the specific heat capacity and the thermal conductivity of paraffin E53 during phase change, however values of those quantities for liquid and solid states are nearly constant but different. A geometric parameter named surface ratio was introduced for better tracking of heat transfer enhancement achieved by inserting of rectangular copper fins along the heating cylinder. The surface ratio can be calculated for different fin types and dimensions and used for assessment and optimization of the melting (charging) and solidification (discharging) characteristics of the observed TES. This approach is useful for prediction of melting/solidification time of the TES, since the functional dependence between the surface ratio and the melting time is easily determined. Numerical simulations conducted for 3-D model gives opportunity to have a detailed insight in changes of quantities such as density, thermal conductivity, velocity and heat flux over the TES volume. In order to verify the utilized numerical approach the results for paraffin temperature change during the TES charging process in the selected point of TES volume, obtained by numerical simulation and experimentally, were compared and showed strong correlation.

Acknowledgment

The authors wish to thank the Serbian Ministry of Education, Science and Technological Development for financing projects III42011, TR 33042 and OI 176006.

Nomenclature

A_{mush} – mushy zone constant, [kgm^{-3}s^{-1}]
d – diameter, [m]
g – gravitational acceleration, [ms^{-2}]
H – total enthalpy of the PCM, [Jkg^{-1}]
h – sensible enthalpy of the PCM, [Jkg^{-1}]
ΔH – latent heat content, [Jkg^{-1}]
k – thermal conductivity, [Wm^{-1}K^{-1}]
L – latent heat, [Jkg^{-1}]
l –length, [m]
n – number of fins, [–]
p – static pressure, [Pa]
$\dot{q}$ – surface heat flux, [Wm^{-2}]
S_M – momentum source term, [Pam^{-1}]
s – thickness, [m]
T – temperature, [K]
t – time, [s]
$\bar{v}$ – velocity vector, [ms^{-1}]
x, z – co-ordinates, [m]

Greek symbols

β – liquid volume fraction
γ – surface ratio
μ – dynamic viscosity, [Pa·s]
ρ – density, [kgm^{-3}]
Φ – energy of dissipation, [Wm^{-3}]

Subscripts

f – fin,
l – liquid,
s – solid

Acronyms

PCM – phase change material
TES – thermal energy storage
DSC – differential scanning calorimeter
UDF – user defined function

References

[1] Waqas, A., *et al.*, Phase Change Material (PCM) Storage for Free Cooling of Buildings – a Review, *Renewable and Sustainable Energy Reviews*, *18* (2013), Feb., pp. 607-625
[2] Ismail, K., *et al.*, Numerical and Experimental Study on the Solidification of PCM around a Vertical Axially Finned Isothermal Cylinder, *Applied Thermal Engineering*, *21* (2001), 1, pp. 53-77
[3] Ahmad, M., *et al.*, Experimental Investigation and Computer Simulation of Thermal Behavior of Wallboards Containing a Phase Change Material, *Energy and Buildings*, *38* (2006), 4, pp. 357-366
[4] Mesalhy, O., *et al.*, Carbon Foam Matrices Saturated with PCM for Thermal Protection Purposes, *Carbon*, *44* (2006), 10, pp. 2080-2088
[5] Zhong, Y., *et al.*, Heat Transfer Enhancement of Paraffin Wax Using Graphite Foam for Thermal Energy Storage, *Solar Energy Materials and Solar Cells*, *94* (2010), 6, pp. 1011-1014
[6] Erek, A., *et al.*, Experimental and Numerical Investigation of Thermal Energy Storage with a Finned Tube, *International Journal of Energy Research*, *29* (2005), 4, pp. 283-301
[7] Mosaffa, A., *et al.*, Approximate Analytical Model for PCM Solidification in a Rectangular Finned Container with Convective Cooling Boundaries, *International Communications in Heat and Mass Transfer*, *39* (2012), 2, pp. 318-324
[8] Al-Abidi, A, *et al.*, Internal and External Fin Heat Transfer Enhancement Technique for Latent Heat Thermal Energy Storage in Triplex Tube Heat Exchangers, *Applied Thermal Engineering*, *53* (2013), 1, pp. 147-156
[9] Castell, A., *et al.*, Natural Convection Heat Transfer Coefficients in Phase Change Material (PCM) Modules with External Vertical Fins, *Applied Thermal Engineering*, *28* (2008), 13, pp. 1676-1686
[10] Mat, S., *et al.*, Enhance Heat Transfer for PCM Melting in Triplex Tube with Internal–External Fins, *Energy Conversion and Management*, *74* (2013), Oct., pp. 223-236
[11] Poling, B., *The Properties of Gases and Liquids*, McGraw-Hill Book Company, New York, USA, 2001
[12] Brent, A., *et al.*, Enthalpy–Porosity Technique for Melting Convection-Diffusion Phase Change: Application to the Melting of a Pure Metal, *Numerical Heat Transfer*, *13* (1988), 3, pp. 297-318
[13] Patankar, S., *Numerical Heat Transfer and Fluid Flow*, McGraw-Hill Book Company, New York, USA, 1980

Paper submitted: July 29, 2015
Paper revised: August 21, 2015
Paper accepted: August 28, 2015